Available online at www.sciencedirect.com
ScienceDirect
Spectrochimica Acta Part A 66 (2007) 394–404
SPECTROCHIMICA ACTA PART A
www.elsevier.com/locate/saa

Vibrational assignment and structure of dibenzoylmethane A density functional theoretical study

S.F. Tayyari [a,*], H. Rahemi [b], A.R. Nekoei [c], M. Zahedi-Tabrizi [d], Y.A. Wang [e]

[a] *Chemistry Department, Khayyam Higher Education, Mashhad 9189747178, Iran*
[b] *Chemistry Department, Urmia University, Urmia, Iran*
[c] *Chemistry Department, Ferdowsi University, Mashhad 91775-1436, Iran*
[d] *Chemistry Department, Alzahra University, Tehran 1993891167, Iran*
[e] *Department of Chemistry, University of British Columbia, Vancouver Y6T 1Z1, Canada*

Received 13 February 2006; received in revised form 1 March 2006; accepted 2 March 2006

Abstract

Molecular structure and vibrational frequencies of 1,3-diphenyl-1,3-propanedione, known as dibenzoylmethane (DBM), have been investigated by means of density functional theory (DFT) calculations. The results were compared with those of benzoylacetone (BA) and acetylacetone (AA), the parent molecule. IR and Raman spectra of DBM and its deuterated analogue were clearly assigned.The calculated hydrogen bond energy of DBM is 16.15 kcal/mol, calculated at B3LYP/6-311++G** level of theory, which is 0.28 kcal/mol more than that of AA. This result is in agreement with the vibrational and NMR spectroscopy results. The molecular stability and the hydrogen bond strength were investigated by applying the Natural Bond Orbital analysis (NBO) and geometry calculations. The theoretical calculations indicate that the hydrogen bond in DBM is relatively stronger than that in BA and AA.

Keywords: Vibrational assignment; Dibenzoylmethane; Intramolecular hydrogen bond; β-Diketone; NBO

1. Introduction

Several naturally occurring β-diketones, such as curcumin (major yellow constituent in turmeric, the ground rhizome of *curcuma longa Linn*) and licodione, 1-(2,4-dihydroxyphenyl)-3-(4-hydroxyphenyl)-1, 3-propanedione (a biosynthetic intermediate isolated from cultured *Glycyrrhiza echinata* L. cells [1], one licorice species), have been shown to exhibit great biological effects. Both curcumin (diferuloylmethane) and licodione exhibit strong antioxidant activities and inhibit carcinogenesis [2,3]. On the other hand another class of DBM derivatives, β-hydroxychalcones compounds, belongs to a rare group of flavonids, have been shown that posses insecticidal and piscicidal properties [4]. Due to antitumor and antiflammatory effects of both curcumin and licodione, the structural analogue DBM and its derivatives have received more attention, especially due to their potential use as a chemopreventive agent [5,6]. Furthermore, because of powerful sunscreen activity of DBM derivatives, some of these compounds have been used in the cosmetic industry as sunscreen agents [7–9].

It is well known that the *cis*-enol form of β-diketones is characterized by a strong intramolecular hydrogen bond [10–13]. The simplest members of this class of compounds are malonaldehyde (MA) and acetylacetone (AA), which have been the subject of many theoretical and experimental studies [14–24]. IR, Raman, NMR, X-ray, neutron, and electron diffraction studies on AA and its derivatives [25–40] indicate that substitution of the methyl groups of AA has a drastic effect on both the position of keto-enol equilibrium and the strength of the intramolecular hydrogen bond. It has been shown that substitution of methyl groups in AA by phenyl groups increases the hydrogen bond strength [35–37]. By means of vibrational spectroscopy [36,37], the following trend in hydrogen bond strength has been obtained:

$$AA < BA < DBM$$

These results are in line with the observation of an increase in proton chemical shift of enolated proton, δOH (in $CDCl_3$),

* Corresponding author. Tel.: +98 511 8780216; fax: +98 511 8438032.
E-mail addresses: Tayyari@ferdowsi.um.ac.ir, sftayyari@yahoo.com (S.F. Tayyari).

1386-1425/$ – see front matter © 2006 Elsevier B.V. All rights reserved.
doi:10.1016/j.saa.2006.03.010

from AA (15.44 ppm) to BA (16.11 ppm) to DBM (16.80 ppm) [35].

The structure and vibrational spectra of DBM have been the subject of a few investigations, which support the existence of a strong intramolecular hydrogen bond of chelating nature in the enol form of this molecule [14,36,37,41–43].

The aim of the present paper is to predict the structure and vibrational spectra (harmonic wavenumbers, and relative intensities for Raman and IR spectra) of DBM by means of density functional theory (DFT) levels. The calculated geometrical parameters for DBM will be compared with X-ray and neutron diffraction result [41,42]. Comparison geometrical parameters of DBM with those of AA and BA gives a clear understanding of substitution effect of phenyl groups (in β position) on structure and hydrogen bond strength of this system. The calculated harmonic force constant of DBM was used for predicting the Raman and IR spectra of deuterated specie. The calculated vibrational frequencies and band assignment are compared with those observed experimentally.

2. Experimental

DBM was obtained from Aldrich Chemical Co. Solutions of DBM in solvents were made with a constant mole ratio of 1 mol of solute to about 20 mol of solvent.

The mid-IR spectra of DBM were recorded by using Bomem MB-154 Fourier Transform Spectrophotometer in the region 500–4000 cm^{-1} in KBr pellet and in CCl_4/CS_2 solution. The spectra were collected with a resolution of 2 cm^{-1} by coadding the results of 16 scans.

The Far-IR spectra in the region 600–50 cm^{-1} were obtained using a Thermo Nicolet NEXUS 870 FT-IR spectrometer equipped with DTGS/polyethylene detector and a solid substrate beam splitter. The spectra were collected with a resolution of 2 cm^{-1} by coadding the results of 128 scans.

The Raman spectra were collected employing a 180° back scattering geometry and a Bomem MB-154 Fourier Transform Raman spectrometer. The Raman spectrometer was equipped with a ZnSe beam splitter and a TE cooled InGaAs detector. Rayleigh filtering was afforded by two sets of two Holographic technology filters. Laser power at the sample was 300 MW. The spectra were collected with a resolution of 2 cm^{-1} by coadding the results of 250 scans.

3. Method of analysis

Geometrical calculations were performed using Gaussian 03 version B05 [44] and NBO 5.0 [45] programs. Geometries of the *cis*-enol forms of DBM are fully optimized with hybrid density functional B3LYP [46,47] using 6-31G**, 6-311G**, and 6-311++G** basis sets. The vibrational frequencies were calculated at B3LYP/6-311G** level of theory. Orbital populations and Wiberg bond orders [48] were calculated with NBO 3.0 program implemented in Gaussian 03. The second order interaction energies (E^2) [49] were performed at the B3LYP/6-311G** level using NBO 5.0 program, which applied the wave function information file generated by earlier version of NBO (3.0).

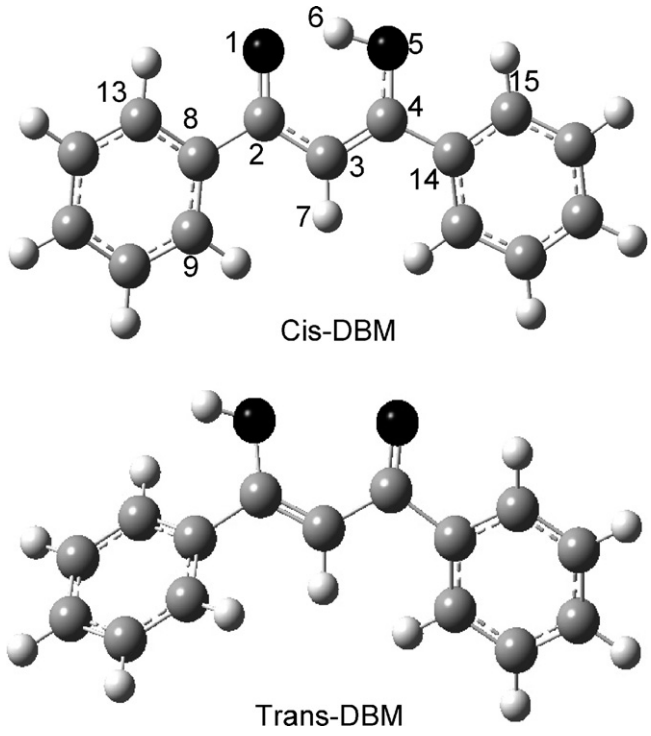

Fig. 1. Numbering system and *cis*- and *trans*-structure of DBM.

The assignment of the experimental frequencies are based on the observed band frequencies and intensity changes in the infrared and Raman spectra of the deuterated species and confirmed by establishing one to one correlation between observed and theoretically calculated frequencies.

4. Results and discussion

4.1. Molecular geometry

The geometry of the *cis*- and *trans*-enol forms along with the atom numbering system are given in Fig. 1. The full optimized geometrical parameters of DBM, AA, 2BA and 4BA [50] along with the reported experimental structural parameters of DBM [41,42] are compared in Table 1.

According to Table 1, substitution of each methyl group by a phenyl group reduces the O···O distance by about 0.02 Å. This result is in agreement with the observed ^{1}H NMR chemical shift, which indicates that by each phenyl substitution the proton chemical shift of the enolated proton shows a downfield by about 0.8 ppm [35]. As it is shown in Table 1, calculations predict a relatively strong hydrogen bond in DBM molecule with an O···O distance of 2.502 Å (calculated at B3LYP/6-311++G** level of theory). This O···O distance is about 0.042 and 0.022 Å shorter than that of AA and 2BA, respectively, which indicates considerably stronger hydrogen bond in DBM compare with that in BA and AA. This result is in agreement with the NMR result [35].

According to Table 1, substitution of the first phenyl group in the enol side, 4BA, increases the C=C and C=O bond lengths by 0.008 and 0.004 Å, respectively, while the C–C bond length

Table 1
The geometrical parameters of the *cis*-enol forms of DBM, BA, and AA calculated at the B3LYP level with 6-311++G** basis set[a]

	Theoretical[b]						Experimental	
	DBM			2BA	4BA	AA	N.D. [41]	X-ray [42]
	A	B	C	C	C	C		
O···O	2.4786	2.5003	2.5024	2.520	2.513	2.544	2.461	2.463
O–H	1.0219	1.0105	1.010	1.006	1.01	1.003	1.257	1.163
H···O	1.5274	1.5686	1.574	1.604	1.585	1.633	1.287	1.362
C=O	1.2618	1.2532	1.254	1.252	1.25	1.246	1.284(3)	1.279
C–O	1.3245	1.3244	1.326	1.324	1.326	1.326	1.292(3)	1.318
C=C	1.3824	1.3782	1.378	1.372	1.378	1.37	1.383(4)	1.394
C–C	1.4375	1.4395	1.439	1.443	1.439	1.444	1.389(4)	1.425
C2–C8	1.4946	1.4959	1.496	1.495	1.478	1.511	1.481(4)	1.477
C4–C14	1.4783	1.478	1.478	1.496	1.511	1.494	1.480(4)	1.477
OHO	152.38	150.89	150.4	148.9	150.5	148.6	150.7	154.7
COH	104.92	105.5	105.8	105.8	106.1	106.2	103.5	102.6
C–C=O	120.86	120.98	120.8	120.5	121.7	121.5	119.9(3)	120.1
C–C=C	119.89	120.31	120.6	120.6	119.2	120.8	121.4(3)	120.4
C=C–O	120.91	121.17	121.1	122.2	121.7	122	120.6(3)	120.3
$\Phi 2$	11.65	11.33	12.0				2.9(4)	
$\Phi 4$	15.55	15.16	14.8				8.8(4)	
H–C=C	119.47	119.25	119.2	121.1	120.6	119.9	119.2	118.9
H–C–C	120.54	120.35	120.3	118.3	120.2	119.3	119.3	120.7
$\Phi 2C2O1$	118.19	118.38	118.5	118.6	114.6	119.9	116.3(3)	117.6
$\Phi 4C4O2$	114.74	114.49	114.5	113.8	119.1	113.8	115.9(3)	115.4

[a] A, B, C, stand for 6-31G**, 6-311G**, and 6-311++G** basis sets, respectively; $\Phi 2$ and $\Phi 4$, phenyl group in the keto and enol sides, respectively; $\phi 2$ and $\phi 4$, O1C2C8C13 and O5C4C14C15 dihedral angles, respectively.
[b] Data for BA and AA from Ref. [50].

decreases by 0.005 Å. Substitution of the second phenyl group, in the carbonyl side, only affects the C=O bond length and changes in the other bond lengths are negligible. These changes in the bond lengths indicate that the π-electron delocalization in the enol ring slightly increases by phenyl substitution in the hydroxyl side. Substitution of phenyl group in the carbonyl side only increases the C=O bond length.

The O···O distance of α-cyano-acetylacetone (CNAA), 2.496 Å [33], is slightly shorter than the corresponding value for DBM, 2.502 Å, which indicates slightly stronger hydrogen bond in CNAA than that in DBM. This conclusion is well supported by the NMR proton chemical shifts of 15.44, 16.11, 16.80 [26], and 16.9 ppm [33] (all in $CDCl_3$) for AA, BA, DBM, and CNAA, respectively.

For comparison, the optimized geometrical parameters of the chelated rings of AA [8], BA, DBM and CNAA [33], all calculated at the B3LYP/6-311++G** level, and some spectroscopic properties, related to their hydrogen bond strength, are listed in

Table 2
Comparing several properties related to the hydrogen bond strength for AA, DBM, BA (averaged), TFAA (averaged), and CNAA[a]

	TFAA [24][b]	AA [17]	BA [50]	DBM	CNAA [33]
δOH	14.2	15.4	16.2	16.8	16.9
νOH	2900	2750	2650	2620	2633
νOD	2120	2020	1960	1950	1970
νOH/νOD	1.37	1.36	1.35	1.34	1.34
γOH	892	952	957	965	993
γOD	650	707	720	720	744
RO···O	2.566	2.544	2.516	2.502	2.496
RC=O	1.237	1.246	1.251	1.254	1.241
RC–O	1.320	1.326	1.325	1.326	1.311
RC=C	1.378	1.374	1.375	1.378	1.391
RC–C	1.426	1.444	1.441	1.439	1.465
RO–H	0.998	1.003	1.008	1.01	1.012
RH···O	1.672	1.635	1.594	1.574	1.570
θOHO	146.8	148.5	149.7	150.4	149.6
E_{HB} (kcal/mol)	12.89	15.87	16.07	16.15	16.26

[a] Frequencies in cm^{-1}, bond lengths in Å, and bond angle in °; δ, proton chemical shift (in ppm); ν, and γ are the stretching and out-of-plane bending, respectively. E_{HB}, difference between the energies of hydrogen-bonded and non-hydrogen-bonded rotamers.
[b] The theoretical parameters is given for the most stable conformer.

Table 3
Selected Wiberg bond orders of DBM, BA and AA calculated at B3LYP/6-311G** level of theory[a]

Bond	DBM	2BA	4BA	AA
O–H	0.6103	0.6205	0.6144	0.6268
C–O	1.1594	1.1670	1.1520	1.1598
C=C	1.4998	1.5403	1.5095	1.5522
C–C	1.2011	1.1870	1.2003	1.1848
C=O	1.5173	1.5309	1.5673	1.5847

[a]Data for AA and BA from Ref. [50].

Table 2. Another parameter, which could be related to the hydrogen bond strength, is the hydrogen bond energy, E_{HB} (the energy difference between the chelated and *trans*-enol rotamers). E_{HB} for AA, BA, DBM, and CNAA are also compared in Table 2 and the following trend in hydrogen bond strength is concluded:

$$AA < BA < DBM < CNAA$$

This trend suggests that the π-systems, such as phenyl and CN groups, increase the H-bond strength through conjugation with the enol ring.

The νOH/νOD ratio has been used as a parameter for estimating the hydrogen bond strength [37]. This parameter is also given in Table 2 and is in excellent agreement with the above trend in the hydrogen bond strength.

4.2. NBO analysis

4.2.1. Bond order

The calculated Wiberg bond orders [48] for DBM along with those for 2BA (phenyl adjacent to the C=O group), 4BA (phenyl in the enol side), and AA, for comparison, are collected in Table 3. According to Table 3, the C=C and C=O bond orders decrease from AA to BA to DBM. By averaging the bond orders for both BA tautomers, one may conclude that by each phenyl substitution the C=C and C=O bond orders reduce more than 0.025 and 0.03, respectively. On the other hand, the C–C bond order slightly increases by increasing the hydrogen bond strength but the C–O bond order is almost constant. Table 3 also shows that the C=C bond order in 2BA is considerably greater than that in 4BA whereas the C=O bond order in 2BA is significantly less than that in 4BA. These results are explainable if we notice that in 2BA the phenyl and C=O groups are adjacent, therefore, a conjugation between C=O and phenyl is expected, however, in 4BA there is a conjugation between the phenyl group and the C=C bond, which results in decreasing the C=C bond order.

Comparing the C–C, C=C and C=O bond orders of DBM, 2BA and 4BA with the corresponding bond orders in AA reveals that substitution of CH_3 groups with phenyl increases the π-electron delocalization in C=C–C=O fragment of the enol ring. The C–O bond order in 4BA is slightly smaller than that in AA. This difference indicates that the resonance of the phenyl group with the π-electron system of the enol ring in 4BA slightly reduces the contribution of C–O bond in this conjugation.

It is noteworthy that the O–H bond order correlates with the calculated O···O distance, by increasing the hydrogen bond strength, reducing the O···O distance, the O–H bond order decreases.

4.2.2. Electron delocalization

Delocalization of electron density between occupied Lewis-type (bond or lone pair) NBO orbitals and formally unoccupied (antibond or Rydberg) non-Lewis NBO orbitals corresponds to a stabilizing donor–acceptor interaction. The energy of these interactions can be estimated by the second order perturbation theory [49].

Table 4 lists the calculated second order interaction energies $E^{(2)}$ between the donor–acceptor orbitals in DBM, 2BA, 4BA, and AA. According to this table, there is no significant difference between the interaction energies of the compared species, except the interaction energies between the phenyl group and C=O and C=C in DBM, 2BA and 4BA. The interaction between the phenyl group and the π^* orbital of the adjacent double bond of the enol ring is relatively large, about 20 kcal/mol. Therefore, stabilization through resonance with the phenyl group is

Table 4
Selected second order perturbation energies $E^{(2)}$ (donor → acceptor)[a]

Donor	Type	Acceptor	Type	DBM	2BA	4BA	AA
C=C	π	C=O	π^*	33.0	32.4	33.4	32.5
C_{14}–C_{15}	π	C=C	π^*	19.1	–	19.6	–
C_8–C_9	π	C=O	π^*	21.8	21.9	–	–
O_5	CR(1)	C_4	$RY^*(1)$	9.9	3.9	5.9	3.8
O_1	CR(1)	C_2	$RY^*(1)$	4.8	5.2	5.9	5.9
O_1	LP(1)	C–C	σ^*	5.4	5.2	5.6	5.3
O_1	LP(2)	C–C	σ^*	8.6	9.1	9.2	9.8
O_1	LP(2)	C_2–$C_{8(9)}$	σ^*	16.4	16.8	17.4	17.8
O_1	LP(2)	O–H	σ^*	35.1	30.8	32.5	28.1
O_5	LP(1)	C=C	σ^*	7.0	7.2	6.9	7.1
O_1	LP(1)	C_2	$RY^*(1)$	9.9	10.2	11.9	12.2
O_5	LP(2)	C=C	π^*	48.6	50.4	48	49.8
C_3–H_7	σ	C–O	σ^*	6.1	6.4	6.0	6.4
O–H	σ	C_4–$C_{8(9)}$	σ^*	5.8	5.9	5.7	5.8

Data for BA and AA from Ref. [50].
[a] Energy in kcal/mol.

Table 5
Selected natural charges (*e*) for optimized *cis*-enol DBM, BA and AA[a]

Atom	DBM	2BA[b]	4BA	BA (averaged)	AA
O_1	−0.653	−0.655	−0.642	−0.649	−0.641
O_5	−0.657	−0.658	−0.663	−0.661	−0.661
C_2	0.519	0.525	0.547	0.536	0.552
C_3	−0.430	−0.455	−0.449	−0.452	−0.475
C_4	0.465	0.490	0.463	0.477	0.486
H_6	0.496	0.496	0.496	0.496	0.495
ΣQ[c]	−0.26	−0.257	−0.248	−0.253	−0.244

[a] All data obtained at B3LYP/6-311G** level of theory.
[b] Data for BA and AA are from Ref. [50].
[c] ΣQ, sum over all enol ring atoms natural charges.

Table 6
Fundamental band assignment of DBM (frequencies are in cm^{-1})[a]

Theoretical[b]					Experimental				Assignment
No.	Freq.	I.IR	I.R	dp	IR (CCl_4)	IR (solid)	R (solid)	R (CCl_4)[c]	
1	3252	2	33	0.15	3134 (vw)	3128 (vw)	3126.1		νCH_α
2	3212	4	106	0.21	3083	3092			2
3	3206	6	121	0.17	3083 (*)	3092	3074 vw		2
4	3196	1	19	0.61	3067 (11)	3061 (m)			20b
5	3196	19	300	0.11	3067 (*)	3061 (*)	3063	3065 (5)	20b
6	3187	31	142	0.29	3067 (sh)	3061 (*)			20a
7	3186	26	202	0.25	3067 (*)	3061 (*)			20a
8	3176	9	145	0.74	3045 (sh)	3045 (sh)			7b
9	3175	11	152	0.74	3045(*)	3045 (sh)			7b
10	3166	0	51	0.71	3034 (sh)	3028 (sh)			13
11	3164	0	54	0.71	3034 (*)	3028 (*)			13
12	2914	456	70	0.23	2620 (vbr)	2595 (vbr)			OH
13	1656	624	524	0.33	1603 (73)	1541 (vs,br)			νaC=C–C=O + δOH + δCH
14	1645	27	545	0.4	1602 (21)	1598 (vs)	1596 (100)	1602 (100p)	8a
15	1644	128	145	0.51	1563 (28)	1541 (*)	1534 (w, br)	1560 (w,br,p)	νsC=C–C=O + δOH + 8a
16	1639	48	443	0.3	1572 (10)	1541 (*)	1534 (*)		δOH + νC=O + 8b
17	1617	151	66	0.29	1563 (*)	1541 (*)	1534 (*)	1560 (*)	δOH + 8b
18	1604	89	127	0.22	1541 (50)	1541 (*)	1534 (*)	1560 (*)	νaC=C–C=O + δOH + δCH + 8b
19	1528	17	20	0.53	1499 (4)				19a
20	1526	38	99	0.32	1488 (13)	1485	1494 (12)	1496 (7 p)	19a
21	1492	227	26	0.47	1468 (29)	1473			νaC–C=C–O + δCH + δOH + 19b
22	1480	18	5	0.44	1435 (6)	1435			19b
23	1456	155	127	0.33	1418 (7, br)	1425	1439 (6)	1446 (3 p)	νaC–C=C–O + δCH + δOH + 19b
24	1376	211	94	0.31	1340(4, vbr)	1339 (w)	1332 (3)		νsC=C–C=O + νsC–C=C–O + δOH + 3
25	1355	13	7	0.54					3
26	1351	18	39	0.42	1305 (23)	1312 (s)			14
27	1335	34	213	0.29	1305 (*)		1308 (10)		νsC=C–C=O + δOH + 14
28	1327	27	6	0.42	1305 (*)				14
29	1306	133	1043	0.29	1280 (16)	1299 (s)	1288 (51)	1282 (44 p)	νsC–C=C + δOH
30	1242	144	36	0.73	1224 (44)	1229 (s)	1229 (2)	1230 (sh,dp?)	δCH + νaC–Φ
31	1207	16	38	0.25	1182 (17)	1193 (vw)	1190 (13)	1188 (18 p)	9a
32	1204	15	40	0.22	1182 (*)	1183 (vw)	1180 (15)	1188 (*)	9a
33	1185	1	11	0.73	1159 (4)	1167 (vw)	1165 (6)	1160 (2 dp)	15
34	1183	3	10	0.75	1159 (*)		1160 (6)	1160 (*)	15
35	1127	8	6	0.47	1102 (5)	1102 (vw)	1104 (1)		δCH + νC–O + νC=O + 18b
36	1109	14	0	0.35	1074 (6)	1092 (vvw)	1091 (vw)		18b
37	1100	14	5	0.39	1074 (*)	1070 (sh)	1072 (vw)	1160 (6)	δCH + 18b
38	1078	53	5	0.3	1064 (13)	1059 (w)	1057 (4)		νsC–C=C + δCH + 18a
39	1050	9	3	0.82	1026 (17)	1029 (w)			18a
40	1044	21	22	0.09	1026 (*)	1023 (w)	1023 (5)	1026 (1)	18a
41	1018	1	88	0.14	1001 (8)		998 (54)	1002 (59 p)	12
42	1017	5	63	0.18	1001 (*)	1000 (w)	998 (*)	1002 (*)	12
43	1016	0	0	0.72					5
44	1012	1	1	0.75	989 (1)	984 (vw)	986 (3)	990 <1	5
45	1002	80	1	0.74	965 (8, br)	970 (w, br)			γOH

Table 6 (*Continued*)

Theoretical[b]					Experimental				Assignment
No.	Freq.	I.IR	I.R	dp	IR (CCl_4)	IR (solid)	R (solid)	R (CCl_4)[c]	
46	992	0	0	0.18					17a
47	989	1	1	0.21			972 (vw)		17a
48	948	2	1	0.24	926 (5)	927 (w)			17b
49	946	0	2	0.37			917 (6)	920 (2)	17b
50	936	1	1	0.1	924 (3, br)				γCCC
51	859	0	1	0.68		851 (vvw)	842 (3)	848 (2 dp)	10a
52	857	0	6	0.21	840 (2)[‡]	842 (vw)			10a
53	829	0	1	0.66					γCH + 10a
54	805	8	4	0.74	810 (3)[‡]	812 (w)			Δ + 6a
55	798	4	9	0.46	786 (14)[‡]	787 (w)	784 (8)	790 (6)	11 + Γ
56	762	126	1	0.57	753 (100)[‡]	756 (vs)	763 (2)		γCH + 11
57	721	12	0	0.22	708 (21)[‡]	706 (m)			11 + γCH
58	706	6	5	0.5	686 (50)	681 (vs)			4
59	701	44	0	0.24	686 (*)				4
60	698	7	8	0.08	686 (*)		678 (10)	684 (8 p)	6b
61	675	1	10	0.44		670 (vw)	666 (2)		Γ + 4
62	635	9	4	0.73	619 (12)	618 (w)			6b + Δ
63	634	0	9	0.74			616 (7)	620 (4 dp)	6b
64	620	38	2	0.72	609 (26)	608 (m)	610 (sh)		Δ + 6b
65	510	15	2	0.34	506 (5)	494 (w)			δCCΦ
66	494	4	9	0.25			487 (5)	493 (6)	νO···O + 16b
67	455	4	1	0.41	448 (mw)	448 (vw)	458 (sh)		νO···O + 16b
68	441	5	1	0.22	448 (*)	448 (*)			16b
69	412	0	2	0.4			425 (1)	406 (4)	16a
70	411	0	1	0.51	402 (w)	399 (w)	400 (4)		16a
71	365	4	1	0.37	363 (m)	361 (w)			Δ
72	333	4	0	0.72			335 (2)	332(sh)	νO···O + δCCΦ
73	237	1	1	0.15	235 (w)				Δ
74	232	1	1	0.73	235 (*)		223 (6)	224 (sh)	Δ
75	196	0	6	0.75	204 (sh)		209 (13)	210 (2)	γCCΦ
76	174	1	2	0.73			172 (vw)		δCCΦ
77	99	0	2	0.75	105 (w)		93 (36)	77	γCCΦ
78	83	0	1	0.53			74 (50)		$\tau\Phi$ + Γ
79	71	0	3	0.69			67 (sh)		δCCΦ
80	30	0	6	0.68			45 (50)		$\tau\Phi$
81	22	0	4	0.74					$\tau\Phi$

[a] IR, infrared; R, Raman; ν, stretching; δ, in-plane bending; γ, out-of-plane bending; Δ, in-plane ring deformation; Γ, out-of-plane ring deformation; v, very; s, strong; m, medium; w, weak; sh, shoulder; τ, torsion; relative intensities are given in parentheses; Φ, phenyl; (*), band overlapped.

[b] Unscaled frequencies calculated at B3LYP level with 6-311G** basis set; I.IR, infrared intensity in KM/mol; I.R, Raman scattering activities in A^4/amu.

[c] Data from Ref. [14].

[‡] CS_2 solution.

expected. This may explain the almost coplanarity of the phenyl and the enol rings in DBM and BA. The observed dihedral angle between the phenyl and the enol rings for BA is only 6° [40] and for DBM are 2.9 and 8.8° [41]. The corresponding calculated dihedral angles for BA, on average, and DBM are 10.8, 12.0 and 14.8°, respectively, which are in good agreement with the experimental results.

It is noteworthy that the $E^{(2)}$ of $LP(2)O_1 \rightarrow \sigma^*$ (O–H) could be well correlated to the O···O distance. The high value of this energy, about 30 kcal/mol for BA and 35 kcal/mol for DBM, indicates that this interaction plays an important role in stabilization of the chelated ring in the enol forms of β-diketones.

4.2.3. Charge analysis

The charge distribution calculated by the NBO method for optimized geometries of DBM, 2BA, 4BA and AA are tabulated in Table 5. As Table 5 indicates, substitution of phenyl for CH_3 groups in AA slightly modifies the charge distribution in the enol ring. The natural charges over O_5 and H atoms in 4BA are almost the same as those in AA. The relatively large charge difference over C_3 and C_4 in 4BA tautomer is caused by conjugation of C=C with the phenyl group. In the case of 2BA this modification in the charge distribution is pronounced for C_2 and O_1 atoms, which confirms existing of significant resonance between the C=O and the phenyl groups. In the case of DBM, due to the conjugation with both C=O and C=C bonds, the charges over C_2, C_3, and C_4 are considerably changed. It is noteworthy that the sum of the charges over all enol ring atoms slightly increases from AA to BA to DBM, which indicates that phenyl groups, in addition to conjugation with the enol double bonds, act as electron donating groups.

Table 7
Fundamental band assignment of D_2DBM (frequencies are in cm^{-1})[a]

No.	Theoretical[b]				Experimental[c]		Assignment
	Freq.	I.IR	I.R	dp	IR (CCl_4)	R (CCl_4)	
1	2400	1	6	0.51			νCD
2	3212	3	104	0.21	3085 (s)		2
3	3206	6	127	0.17	3085		2
4	3197	15	206	0.13	3065 (m)	3064 (5)	20b
5	3196	5	86	0.13	3065	3064	20b
6	3187	23	200	0.25	3065	3064	20a
7	3186	34	171	0.24	3065	3064	20a
8	3176	10	146	0.74	3025 (sh)		7b
9	3175	11	155	0.74	3025		7b
10	3166	0	51	0.71			13
11	3164	0	54	0.72			13
12	2136	350	8	0.24	1950 (w,br)		νOD
13	1646	44	304	0.38	1600 (s)	1600 (100)	νaC=C–C=O + 8a
14	1645	9	597	0.40	1600 (*)	1600 (*)	8a
15	1639	124	167	0.44	1600 (*)	1600 (*)	νaC=C–C=O + 8b
16	1623	10	33	0.36	1575 (w)		8b
17	1601	271	22	0.42	1565 (s)		νaC=C–C=O + 8b
18	1540	331	969	0.30	1520 (vs)	1504 (45 p)	19a
19	1525	21	53	0.33			19a
20	1513	511	397	0.28	1483 (s)	1486 (8 p)	νsC=C–C=O + 19a
21	1480	78	12	0.75	1443 (mw)		19b
22	1474	45	256	0.31		1448 (7 p)	19b
23	1398	63	30	0.37	1365 (w)	1370 (3 p)	νaC–C=C–O + 3
24	1356	28	50	0.29	1322 (ms)		3
25	1353	18	50	0.32			3
26	1344	148	173	0.29			νsC–C=C–O + 14
27	1327	53	19	0.31			+νsC–C=C–O + 14
28	1320	80	135	0.30	1295 (ms)	1296 (4 p)	νsC–C=C + 14
29	1208	4	22	0.26	1180 (w)	1184 (10 p)	9a
30	1205	4	9	0.36	1180 (*)	1184 (*)	9a
31	1188	52	16	0.60	1170 (s)	1176 (1 dp)	νaC-Φ + 9b
32	1185	0	12	0.69		1176 (*)	15
33	1182	14	16	0.75	1158 (w)	1160 (3 p)	15
34	1127	51	302	0.42	1080 (m)	1088 (28 p)	δOD + νC=C + 19a
35	1109	18	0	0.42	1098 (sh)		18b
36	1107	13	3	0.54	1098 (*)		18b
37	1068	47	71	0.24	1040	1042 (28 p)	δOD + νsC–C=C + 19a
38	1050	10	2	0.51	1028 (m)		18a
39	1041	38	7	0.15	1019 (m)		18a
40	1018	1	64	0.14	1001 (m)	1000 (88 p)	12
41	1017	4	78	0.16	1001 (*)	1000 (*)	12
42	1016	0	1	0.43			5
43	1012	0	1	0.74			5
44	992	1	0	0.17		990 (1)	17a
45	989	1	2	0.21	975 (vw)		17a
46	948	1	1	0.69	926 (w)		17b
47	946	1	1	0.66	926		17b
48	901	10	9	0.14	878 (w)		δCD + νC–O + nC-F
49	887	4	9	0.36	850 (w)		δCCC + δOD
50	859	1	4	0.30			10a
51	856	0	3	0.26			10a
52	832	3	6	0.44	805 (w)		10b
53	798	3	3	0.71	780 (mw)		10b
54	792	5	3	0.63	780	788 (vw)	Δ + 6a
55	755	142	0	0.57	730 (s)		11 + γOD
56	714	45	2	0.43	720 (m)		γOD + 11
57	706	5	3	0.69			11
58	698	24	0	0.20	688 (s)		4
59	695	9	9	0.10	688	680 (12 p)	6a
60	673	0	4	0.71			Γ + 4
61	634	5	5	0.74	618 (mw)	620 (4 dp)	6b

Table 7 (*Continued*)

No.	Theoretical[b]				Experimental[c]		Assignment
	Freq.	I.IR	I.R	dp	IR (CCl_4)	R (CCl_4)	
62	634	0	8	0.73	618	620	6b
63	614	40	1	0.69	600 (m)		Δ + 6a
64	567	5	3	0.21	562 (m)		γCD
65	497	11	3	0.34	495 (mw)		Δ + δCCF
66	491	7	9	0.28	495	498 (w,br)	νO···O + δCCΦ
67	454	9	0	0.19	448 (mw)		νO···O + 16b
68	435	1	1	0.71	400 (w)		16b
69	412	0	1	0.75			16a
70	411	0	2	0.43		406 (w)	16a
71	362	5	1	0.34	351 (m)		Δ
72	327	4	1	0.52		325 (w)	νO···O + δCCΦ
73	235	1	1	0.17	231 (w)		Δ
74	221	1	3	0.67		222 (vw)	Δ
75	200	0	4	0.64		206 (vw)	γCCΦ
76	176	1	4	0.75	200 (w)		δCCΦ
77	95	0	3	0.73	105 (w)		γCCΦ
78	80	0	2	0.46		77	$\tau\Phi$ + Γ
79	71	0	3	0.55			δCCΦ
80	30	1	5	0.69			$\tau\Phi$
81	24	0	2	0.74			$\tau\Phi$

[a] IR, infrared; R, Raman; ν, stretching; δ, in-plane bending; γ, out-of-plane bending; Δ, in-plane ring deformation; Γ, out-of-plane ring deformation; v, very; s, strong; m, medium; w, weak; sh, shoulder; τ, torsion; Φ, phenyl; p, polarized; dp, depolarized.

[b] Unscaled frequencies calculated at B3LYP level with 6-311G** basis set I.IR, infrared intensity in KM/mole; I.R, Raman scattering activities in A^4/AMU.

[c] Data from Ref. [14].

4.3. The computed vibrational spectra and interpretation of the experimental spectra

The assignments of the experimental frequencies are based on the observed band frequencies and intensity changes in the infrared and Raman spectra of the deuterated species confirmed by establishing one to one correlation between observed and theoretically calculated frequencies.

The IR and Raman band frequencies for DBM and D_2DBM in the solid phase and in solutions along with the calculated frequencies and their assignments are given in Tables 6 and 7, respectively. The IR and Raman spectra of DBM in the solid state are shown in Figs. 2 and 3, respectively.

Lorentzian function has been utilized for deconvolution of the IR spectrum of DBM in the 1700–800 cm^{-1} region and it is shown in Fig. 4.

Assignments for phenyl group are given in Wilson's notation [51]. The calculated frequencies are slightly higher than the observed values for the majority of the normal modes. In addition to the error of the theoretical method used, the difference between the computed and experiment frequencies may be due to many different factors that are usually not even considered in the theory, such as anharmonicity, Fermi resonance, solvent effects, etc.

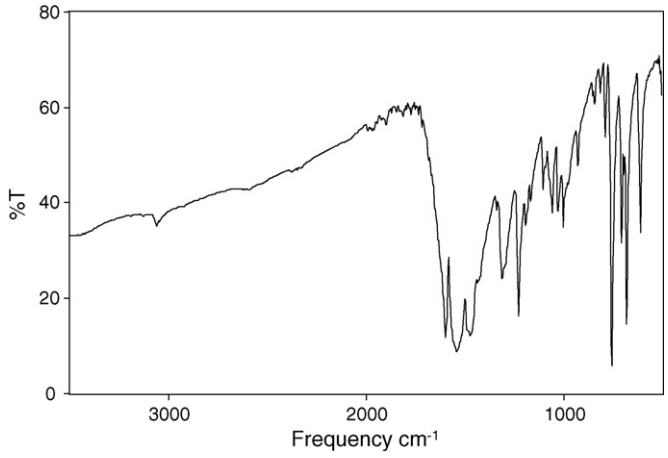

Fig. 2. IR spectrum of DBM in solid phase.

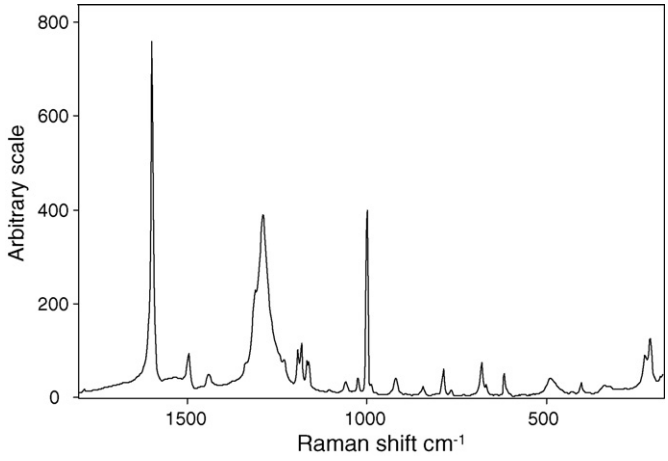

Fig. 3. Raman spectrum of DBM in solid phase.

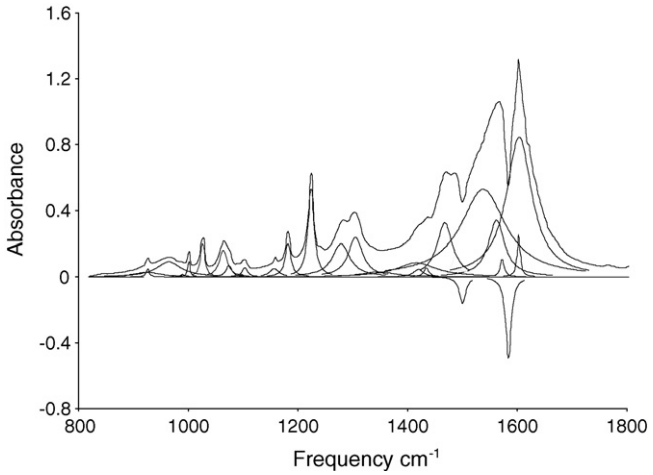

Fig. 4. The deconvoluted infrared spectrum of DBM in CCl_4.

4.3.1. CH and OH stretching region

A very weak band at 3126 cm^{-1} is assigned to the α-CH stretching mode. The corresponding band in AA and BA are observed at 3090 cm^{-1} [17] and 3110 cm^{-1} [50], respectively. Increasing the α-CH stretching upon substitution of CH_3 groups by phenyl groups indicates that phenyl acts as an electron releasing group, therefore, increases the C–H_α strength. This explanation is in agreement with increasing the total charge of the enol ring from AA to BA to DBM (see Table 5).

In the mono-substituted benzene ring, the vibrational modes 2, 20a and 20b are expected to be observed in the 3105–3035 cm^{-1} region [52]. By considering the computed results, the medium IR band at 3067 cm^{-1} with three shoulders at bands 3083, 3045, and 3034 cm^{-1}, as it is given in Table 6 are attributed to the normal modes of phenyl CH stretching movements.

The characteristic OH stretching in the enol form of β-diketones appears as a weak and very broad band at the 3300–2000 cm^{-1} region [17,24,36,37]. The intensity and broadness of this band are depended on the strength of the intramolecular hydrogen bond. Upon increasing the hydrogen bond strength its intensity decreases while its broadness considerably increases [37,53,54]. This band in the IR spectrum of DBM in CCl_4 is centered at about 2620 cm^{-1}. Upon deuteration this band disappears and a new band with considerably narrower band width appears at about 1950 cm^{-1}, which indicates a νO–H/νO–D ratio of 1.34 [37]. The lower frequencies of νOH and νOD and the lower ratio of νO–H/νO–D for DBM in comparison with the corresponding values for AA (1.36) and BA (1.35) confirms stronger hydrogen bond in DBM compared with that in AA and BA. The νO–H/νO–D bands in AA and BA appear at 2800/2027 and 2650/1960 cm^{-1}, respectively [17,50].

4.3.2. 1700–1000 cm^{-1} region

In this region we expect to observe the band frequencies related to the C–C, C=C, C–O, C=O stretching, OH and C–H in-plane bending movements of the enol ring, and the C–C stretching and C–H in-plane bending of the phenyl groups.

The infrared spectrum of DBM, as that of BA [50] and several other β-diketones [17,36,37], apparently shows only one broad band in the C=O and C=C region. This band in the CCl_4 solution of DBM appears at about 1600 cm^{-1}. Deconvoluted infrared spectrum of DBM in this region, Fig. 4, indicates five bands at 1603, 1602, 1572, 1563, and 1541 cm^{-1} (see Fig. 4). Existing of two strong Fermi windows, shown by negative peaks in Fig. 4, makes this region of IR spectrum more complicated. The sharp band at 1602 cm^{-1}, which is not affected by deuteration, is clearly assigned to the C–C stretching of the phenyl group 8a. This band is overlapped with a very strong and broad band due to the asymmetric C=C–C=O stretching strongly interacted with 8b. The corresponding band in the solid state appears at about 1540 cm^{-1}. The phase sensitivity of this band confirms the assignment, since it is shown that this mode of vibration is very phase sensitive [17]. For example, the corresponding band in the gas, liquid, and solid phases of AA appears at 1642, 1625, and 1600 cm^{-1}, respectively. Comparison between the band at 1603 cm^{-1}, ν_aO=C–C=C, with the corresponding band in BA [50], 1618 cm^{-1}, and AA [17], 1625 cm^{-1}, shows that the asymmetric C=C–C=O frequency is shifted toward lower frequencies upon increasing the hydrogen bond strength. The frequency shift by replacing of methyl by phenyl groups could be attributed to the enhancement of π-electron conjugation in the enol ring.

According to the theoretical calculations, the strong band at 1563 cm^{-1} is caused by symmetric C=C–C=O stretching which is coupled to δOH, and 8a. This band is overlapped by another band due to νC=C coupled with δOH and 8b. Upon deuteration the former shifts toward lower frequencies and appears at 1504 cm^{-1}. The observed frequency shifts for AA [17] and BA [50] are about 90 and 75 cm^{-1}, respectively. This frequency shift upon deuteration is due to the removing of the δOH contribution in this mode of vibration and is characteristic for the vibrational spectra of β-diketone systems [16,17,26–28,37,50].

By considering the theoretical calculations and comparing the vibrational spectra of DBM with that of BA, the band at 1487 cm^{-1} is assigned to ν_aO–C=C–C coupled to 19b and δOH. This band is also overlapped with 19a of the phenyl groups.

Upon deuteration a very strong and broad Raman band at 1282 cm^{-1} disappears and two new strong bands appear at 1088 and 1042 cm^{-1}. The 1282 cm^{-1} band is assigned to δOH and symmetric C=C–C stretching. The Raman activity of this band depends on the hydrogen bond strength, stronger hydrogen bond exhibits stronger Raman band [36,37]. According to the calculations, both relatively strong bands at 1088 and 1041 cm^{-1} in the Raman spectrum of DBM have δOD and νC=C characters and both of them are coupled to 19a of the phenyl groups.

The strong IR band at 1229 cm^{-1} is assigned to δCH_α, which upon deuteration disappears. According to the calculations, the weak IR band at 878 m^{-1} is assigned to the corresponding band in deuterated analogue.

The strong Raman band at about 1000 cm^{-1} is attributed to the 12 mode of the phenyl groups.

4.3.3. Below 1000 cm^{-1}

In this region we expect to observe the vibrational band frequencies due to the O–H and C–H out-of-plane bending, and

phenyl and chelated rings in-plane and out-of-plane deformational modes.

The medium and broad band at about 965 cm^{-1} is correlated with the theoretical band at 1002 cm^{-1}, which is assigned to the O–H out-of-plane bending mode. Upon deuteration, this band disappears and a new band appears at about 720 cm^{-1}. The corresponding bands in AA/D_2AA [17] and BA/D_2BA [50] appear at about 950/707 and 960/720 cm^{-1}, which are lower than that for DBM/D_2DBM. The occurrence of γOD in BA and DBM at the same wavenumber could be attributed to the interaction between γOD and 11 in D_2DBM. The higher value of γOH/γOD in DBM in compare with that in BA and AA also supports stronger hydrogen bond in DBM than that in AA and BA.

The strongest band in the IR spectrum of DBM occurs at 753 cm^{-1}, which is attributed to γCH, which is strongly coupled with 11 of the phenyl groups. Upon deuteration γCD moves to 562 cm^{-1} and 11 appears at 730 cm^{-1}, which the latter is now coupled with γOD.

The strong Raman band at 688 cm^{-1} is attributed to one of the in-plane enol ring deformation. The corresponding band in BA and AA appears at considerably lower frequency, 672 and 640 cm^{-1}, respectively. This result is also consistent with the stronger hydrogen bond in DBM compared with that in BA and AA.

According to the calculations, the O···O stretching mode in the DBM is strongly coupled to C–C-phenyl bending and 16b mode of phenyl groups. The only observed IR band due to this mode is the band at 448 cm^{-1}. The corresponding band for BA [50] and AA [17] occurs at 396 and 366 cm^{-1}, respectively. These observations are also confirm stronger hydrogen bond in DBM compared with that in AA and BA.

5. Conclusion

The geometry of DBM is fully optimized at B3LYP (DFT) level of theory using 6-31G**, 6-311G**, and 6-311++G** basis sets. The geometrical parameters are in good agreement with the X-ray and neutron diffraction results.

Comparison of the vibrational spectra and structural parameters of DBM with those of BA and AA reveals a considerably weaker H-bond in AA than that in BA and DBM. The observed OH/OD stretching and OH/OD out-of-plane bending modes are in good agreement with the calculated O···O distances and observed NMR results.

Acknowledgement

We are grateful to the Khayyam Higher Education Center (Mashhad) for its support of this research.

Y.A.W. gratefully acknowledges the financial support from Natural Sciences and Engineering Research Council (NSERC) of Canada.

References

[1] T. Furuya, S.I. Ayabe, M. Kobayashi, Tetrahedron Lett. 29 (1976) 2539.
[2] M.T. Huang, H.L. Newmark, K. Frenkel, J. Cell. Biochem. 27 (1997) 26.
[3] C.V. Rao, A. Riven, B. Simi, B.S. Reddy, Cancer Res. 55 (1995) 259.
[4] F. Gomez-Garibay, J.S. Calderon, L. Quijano, O. Tellez, M. Socorro-Olivares, T. Rios, Phytochemistry 46 (2001) 1285.
[5] C.C. Lin, C.T. Ho, M.T. Huang, Proc. Natl. Sci. Counc. ROC (B) 25 (2001) 158.
[6] M.T. Huang, Y.R. Lou, J.G. Xie, W. Ma, Y.P. Lu, P. Yen, B.T. Zhu, H. Newmark, C.T. Ho, Carcinogenesis 19 (1998) 1697.
[7] F. Wetz, C. Routaboul, D. Lavabre, J.C. Garrigues, I. Rico-Lattes, I. Pernet, A. Denis, Photochem. Photobiol. 80 (2004) 316.
[8] N.M. Rocher, M.K.O. Lindemann, S.B. Kong, C.G. Cho, P. Jiang, J. Photochem. Photobiol. A: Chem. 80 (1994) 417.
[9] W. Schwack, T. Rudolph, J. Photochem. Photobiol. B: Biol. 28 (1995) 229.
[10] A.H. Lowery, C. George, P.D. Antonio, J. Karle, J. Am. Chem. Soc. 93 (1971) 6399.
[11] R.S. Brown, A.T. Nakashima, R.C. Haddon, J. Am. Chem. Soc. 101 (1979) 3175.
[12] J. Emsley, Struct. Bond. 57 (1984) 1.
[13] F. Hibbert, J. Emsley, Hydrogen Bonding and Chemical Reactivity Advanced in Physical Chemistry, vol. 26, Academic Press, London, 1990, p. 255.
[14] S.F. Tayyari, Ph.D. Thesis, London University, 1978.
[15] R. Bose, M.Y. Antipin, D. Bläser, K.A. Lyssenko, K.A. Lessen, J. Phys. Chem. B 102 (1998) 8654.
[16] S.F. Tayyari, M. Zahedi-Tabrizi, F. Tayyari, F. Milani-Nejad, J. Mol. Struct. (Theochem) 637 (2003) 171.
[17] S.F. Tayyari, F. Milani-Nejad, Spectrochim. Acta 56A (2000) 2679.
[18] A.L. Andreassen, D. Zebelman, S.H. Bauer, J. Am. Chem. Soc. 93 (1971) 1148.
[19] A.H. Lowry, C.G.P. D'Antonio, J. Karle, J. Am. Chem. Soc. 93 (1971) 6399.
[20] A. Camerman, D. Mostopaolo, N. Camerman, J. Am. Chem. Soc. 105 (1983) 1584.
[21] D.P. Tew, N.C. Handy, S. Carter, Mol. Phys. 102 (2004) 2217.
[22] K. Iijima, A. Onhogi, D. Shibata, J. Mol. Struct. 156 (1987) 111.
[23] R.D.G. Jones, Acta Crystallogr. B 32 (1976) 2133.
[24] M. Zahedi-Tabrizi, F. Tayyari, Z. Moosavi-Tekyeh, S.F. Tayyari, Spectrochim. Acta, in press.
[25] V.B. Delchev, G.St. Nikolov, Monatsh. Chem. 132 (2001) 339.
[26] S.F. Tayyari, F. Milani-Nejad, Spectrochim. Acta 54A (1998) 255.
[27] S.F. Tayyari, F. Milani-Nejad, H. Rahemi, Spectrochim. Acta 58A (2002) 1669.
[28] S.F. Tayyari, S. Salemi, M. Zahedi-Tabrizi, M. Behforouz, J. Mol. Struct. 694 (2004) 91.
[29] T. Chiavassa, P. Verlaque, L. Pizalla, P. Roubin, Spectrochim. Acta 50A (1993) 343.
[30] T. Chiavassa, P. Roubin, L. Pizalla, P. Verlaque, A. Allouche, F. Marinelli, J. Phys. Chem. 96 (1992) 659.
[31] G. Buemi, J. Mol. Struct. (Theochem) 499 (2000) 21.
[32] V. Bertolasi, P. Gilli, V. Ferretti, G. Gilli, J. Am. Chem. Soc. 113 (1991) 4917.
[33] S.F. Tayyari, F. Milani-Nejad, I.S. Butler, Vibrat. Spectrosc. 26 (2001) 187.
[34] J. Tollec, in: Z. Rappoport (Ed.), The Chemistry of the Enols, John Wiley & Sons, New York, 1990, p. 366.
[35] M. Bassetti, G. Cerichelli, B. Floris, Gazz. Chim. Ital. 116 (1986) 579.
[36] S.F. Tayyari, Th. Zeegers-Huyskens, J.L. Wood, Spectrochim. Acta 35A (1979) 1265.
[37] S.F. Tayyari, Th. Zeegers-Huyskens, J.L. Wood, Spectrochim. Acta 35A (1979) 1289.
[38] M. Gorodetsky, Z. Luz, Y. Mazur, J. Am. Chem. Soc. 89 (1967) 1183.
[39] G.K.H. Madsen, B.B. Iversen, F.K. Larsen, M. Kapon, G.M. Reisner, F.H. Herbstein, J. Am. Chem. Soc. 120 (1998) 10040.
[40] F.H. Herbstein, B.B. Iversen, M. Kapon, F.K. Larsen, G.K.H. Madsen, G.M. Reisner, Acta Crystallogr. B 55 (1999) 767.
[41] B. Kaitner, Acta Crystallogr. C 49 (1993) 1523.
[42] R.D.G. Jones, Acta Crystallogr. B 32 (1976) 1807.
[43] D.E. Williams, Acta Crystallogr. 21 (1966) 340.

[44] M.J. Frisch, G.W. Trucks, H.B. Schlegel, G.E. Scuseria, M.A. Robb, J.R. Cheeseman, J.A. Montgomery Jr., T. Vreven, K.N. Kudin, J.C. Burant, J.M. Millam, S.S. Iyengar, J. Tomasi, V. Barone, B. Mennucci, M. Cossi, G. Scalmani, N. Rega, G.A. Petersson, H. Nakatsuji, M. Hada, M. Ehara, K. Toyota, R. Fukuda, J. Hasegawa, M. Ishida, T. Nakajima, Y. Honda, O. Kitao, H. Nakai, M. Klene, X. Li, J.E. Knox, H.P. Hratchian, J.B. Cross, V. Bakken, C. Adamo, J. Jaramillo, R. Gomperts, R.E. Stratmann, O. Yazyev, A.J. Austin, R. Cammi, C. Pomelli, J.W. Ochterski, P.Y. Ayala, K. Morokuma, G.A. Voth, P. Salvador, J.J. Dannenberg, V.G. Zakrzewski, S. Dapprich, A.D. Daniels, M.C. Strain, O. Farkas, D.K. Malick, A.D. Rabuck, K. Raghavachari, J.B. Foresman, J.V. Ortiz, Q. Cui, A.G. Baboul, S. Clifford, J. Cioslowski, B.B. Stefanov, G. Liu, A. Liashenko, P. Piskorz, I. Komaromi, R.L. Martin, D.J. Fox, T. Keith, M.A. Al-Laham, C.Y. Peng, A. Nanayakkara, M. Challacombe, P.M.W. Gill, B. Johnson, W. Chen, M.W. Wong, C. Gonzalez, J.A. Pople, Gaussian 03, Revision B.05, Gaussian, Inc., Wallingford, CT, 2004.

[45] E.D. Glendening, J.K. Badenhoop, A.E. Reed, J.E. Carpenter, J.A. Bohmann, C.M. Morales, F. Weinhold NBO 5.0. (Theoretical Chemistry Institute, University of Wisconsin, Madison, WI, 2001); http://www.chem.wisc.edu/∼nbo5.

[46] A.D. Becke, J. Chem. Phys. 98 (1993) 5648.

[47] C. Lee, W. Yang, R.G. Parr, Phys. Rev. B 37 (1988) 785.

[48] K.W. Wiberg, Tetrahedron 24 (1968) 1083.

[49] A.E. Reed, L.A. Curtiss, F. Weinhold, Chem. Rev. 88 (1988) 899.

[50] S.F. Tayyari, J.S. Emampour, M. Vakili, A.R. Nekoei, M. Hassanpour, J. Mol. Struct., in press.

[51] E.B. Wilson, Phys. Rev. 4 (1934) 706.

[52] N.B. Colthup, L.H. Daly, S.E. Wiberley, Introduction to Infrared and Raman Spectroscopy, Academic Press, Inc., 1975.

[53] D.N. Shigorin, M.M. Shemykin, M.N. Kolosov, Dokl. Akad. Nauk. SSSR 108 (1956) 672.

[54] D.N. Shigorin, E.A. Gastillovich, T.S. Kopteva, M.M. Victorova, Ah. Fiz. Khim. 42 (1968) 1231.